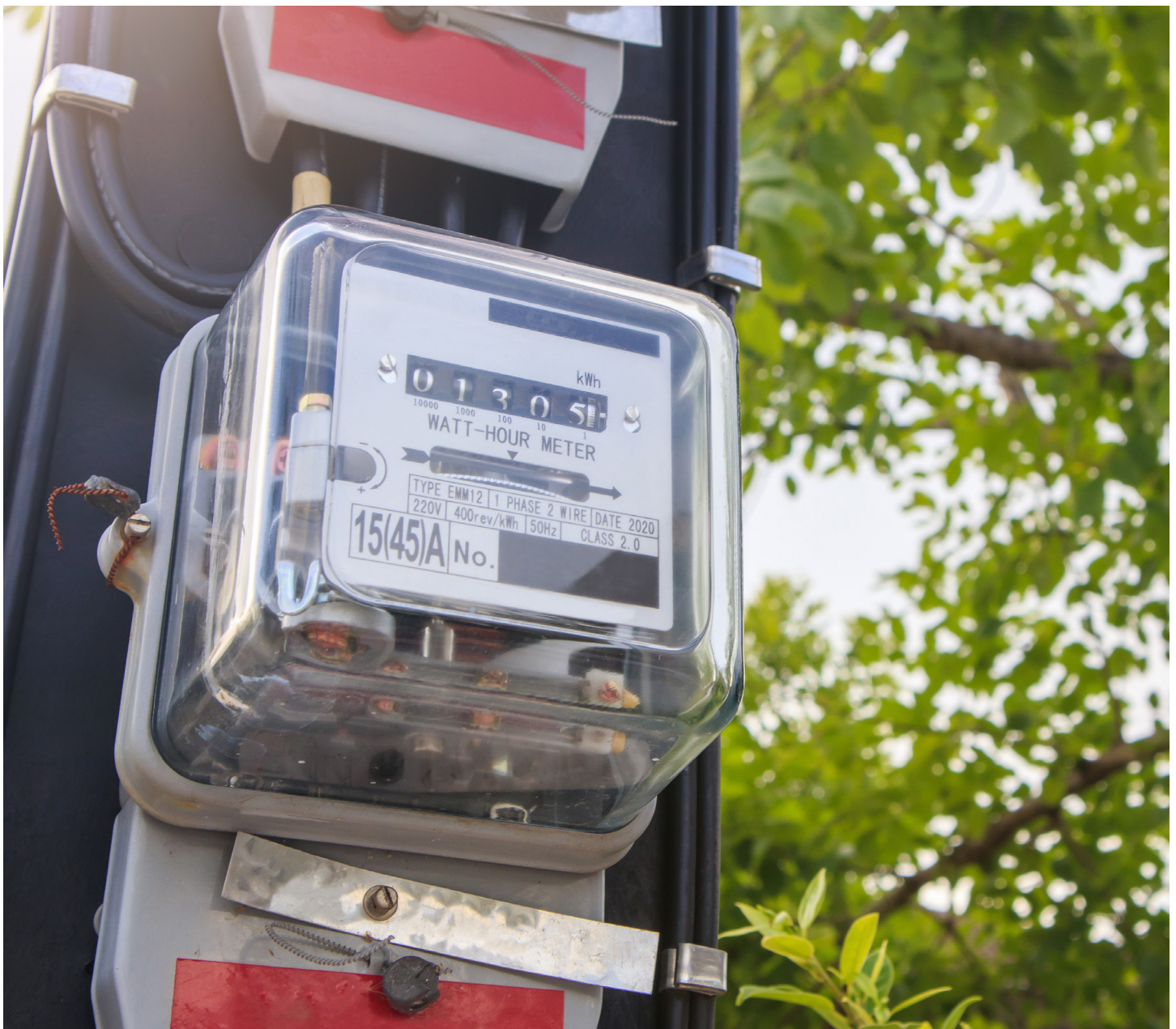


# Multi-Output Flyback Converter for Metering Applications that Protects Against Magnetic Interference

Thomas Anthony Capobianco, Ray Patrick Almeda | Power Integrations, USA



---

## Abstract

Multi-output flyback designs address numerous low-power applications. Integrated devices allow for ease of design while also improving protection. A wide input range, acceptable output regulation, and low no-load input power are common requirements. For metering, there is also a need for equipment to withstand external tampering.

A design method for reducing the susceptibility of the power stage to externally applied magnetic interference is discussed. Appropriate transformer design, component selection, and leveraging the benefits of ON/OFF control help achieve this. Results show start-up waveforms and thermal data. Efficiency, and no-load input power with and without the imposition of strong external magnetic disturbances are compared.

## 1. Introduction

Transformer design is at the core of flyback converter performance regardless of the intended application. Its construction contributes greatly not only to overall converter efficiency but also to electromagnetic compatibility (EMC). Using a power switch combined with the controller inside one package helps streamline the design and reduce component count. Transformer construction, primary switch selection, and control scheme choice are all critical in meeting performance requirements. These also determine how susceptible circuits are to external magnetic fields.

## 2. Magnetic Interference

### 2.1 Electromagnetic Quantities

What happens when you place a permanent magnet close to the transformer of a flyback converter?

Transformers allow the storage and transfer of energy. They can be modeled and analyzed like any magnetic circuit. However, the analysis becomes less intuitive and needs to be modified when an external magnetic field is incident to an already operating transformer. To explain the phenomenon, a review of the basic principles of electromagnetism is necessary.

Magnetic field intensity,  $H$ , and magnetic flux density,  $B$ , are terms that may be mistaken for one another despite having distinct definitions.

Magnetic field intensity, a vector quantity, measures the strength of a field on a point in space. It is defined by the Biot-Savart law [6] in Eq. (1) and has units of amperes per meter. This shows an inverse square dependence on distance and a linear relationship between source and field.

$$H = \oint \frac{IdL \times a_R}{4\pi R^2} \quad (1)$$

Magnetic flux density, a scalar quantity on the other hand, is a measure of the amount of flux per unit area. It has units of Tesla, Webers per meter squared, or Gauss, and can be visualized as the number of imaginary flux lines normal to and passing through an enclosed area. The magnetic flux is the surface integral of the magnetic flux density within an enclosed area [6] as shown in Eq. (2).

$$\Phi = \int_S B \cdot dS \quad (2)$$

---

Magnetic field intensity and magnetic flux density are related by Eq. (3) [6]. It states that the magnetic flux density is directly proportional to the magnetic field intensity, scaled by the permeability of a material,  $\mu$  which has units of Henrys per meter.

$$B = \mu H \quad (3)$$

Having mentioned magnetic flux, the inductance [6] as in Eq. (4) is now defined as the ratio of the total flux linkages to the current which they link. The current  $I$  flowing through the  $N$ -turn coil produces a total magnetic flux ( $\Phi$ ) and has units of Henrys.

$$L = \frac{N\Phi}{I} \quad (4)$$

## 2.2 Magnetic Materials

Permanent magnets exert forces on each other, as well as on pieces of iron that are not magnetized. An object that contains iron but is not itself magnetized (shows no tendency to point north or south) is attracted by either pole of a permanent magnet. A bar magnet sets up a magnetic field in the space around it and a second body responds to that field [1].

Magnetic materials include ferromagnetic, antiferromagnetic, paramagnetic, and diamagnetic material [1]. In power supplies, ferrite cores that are ferrimagnetic material are used due to their inherent properties favorable for switching at high frequencies. When a permanent magnet is placed close to a ferrimagnetic material, as in Eq. (3), relating magnetic flux density, magnetic field intensity, and permeability can be rewritten as Eq. (5) where  $M$  is the magnetization.

$$B = \mu(H + M) \quad (5)$$

The magnetization is dependent on the magnetic material used, the strength of the permanent magnet, and its position relative to a transformer.

When an external magnet is placed close to the transformer, the internal magnetic dipoles of the ferrite core align in an anti-parallel fashion. The magnitude of the resultant magnetic moment, therefore, decreases [1].

If the magnetic moment decreases, the magnetic field intensity  $H$  decreases. A decrease in the magnetic field intensity  $H$  also translates to a decrease in magnetic flux density  $B$ . Accounting for the change in permeability due to magnetization, Eq. (5) can be rewritten as Eq. (6):

$$\downarrow B = \mu_{NEW} \downarrow H \quad (6)$$

## 2.3 Effect of Permanent Magnet on the Transformer

Equation (4) for inductance can be rewritten as Eq. (7) in terms of the magnetic flux density  $B$ , and the effective area  $A$ . In flyback design, both quantities are in the datasheet of the core, chosen depending on the application:

$$LI = NBA \quad (7)$$

The peak current  $I$  through the winding is dependent on both the power MOSFET and the control scheme. The number of turns  $N$ , and the effective area  $A$  physically cannot change. Therefore, a decrease in the magnetic flux density  $B$  due to the presence of an external magnet translates directly to a decrease in the inductance value  $L$ .



**Fig.1 A permanent magnet is placed next to the transformer while the primary inductance is being measured (magnet orientation #1).**

A permanent magnet was placed incident on a transformer. The inductance was measured with varying degrees of closeness and angle. Shown in Table 1 are the measured inductance values.

Magnet Orientation	Magnetizing Inductance (mH)	% Reduction
No magnet	2.61	0
1	1.06	59
2	1.17	55
3	0.90	65
4	1.08	59
5	1.82	30

**Table 1 Primary inductance measured with placement of a permanent magnet near the transformer in different orientations.**

### 3. Flyback Converter Design

When a permanent magnet is close enough to a transformer in an operating power supply, a decrease in inductance is inevitable. The only question that remains is how much of a reduction can the flyback withstand before it is unable to operate continuously. Control scheme and power MOSFET selection determines the peak current  $I$  through the winding and the system response. And the transformer design determines the primary inductance value  $L$ . Therefore, to comply with magnetic interference requirements, power MOSFET selection, control scheme, and transformer design are critical.

#### 3.1 Power MOSFET and ON/OFF Control

LinkSwitch™-XT2 900 V from Power Integrations® was chosen for its ease of design, robustness, and the simple ON/OFF control scheme. Its MOSFET has a breakdown voltage of at least 900 V, which is ideal for the wide input range for the target metering application. With internal peak current limiting of up to 518 mA and maximum switching frequency of 66 kHz, a 6.6 W flyback converter was designed.

Aside from the power device, it is combined with the controller in the same package, which streamlines the design and reduces the component count. The controller utilizes a proprietary ON/OFF control scheme and provides various built-in protection features.

In ON/OFF control, the output voltage is examined before each switching cycle. If the voltage is below a certain threshold, a switching request is initiated, and power MOSFET turns on during that cycle. If the voltage exceeds the threshold, the no switching request is sent, and that switching pulse is skipped. This is examined during every clock cycle and is illustrated in Fig. 2.

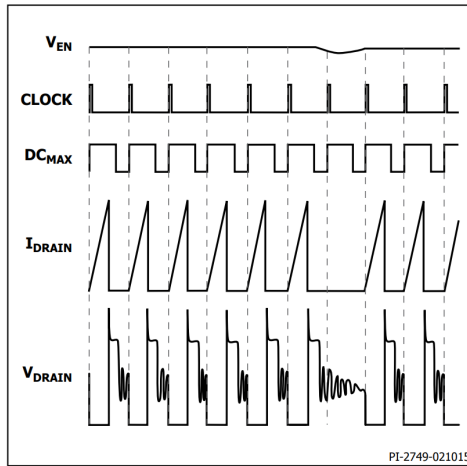


Fig. 2 ON/OFF control operation

### 3.2 Transformer Design

The potential decrease of the primary inductance because of the presence of an external magnet can be addressed by designing with higher target maximum magnetic flux density B<sub>MAX</sub>. Despite designing with higher B in mind, B<sub>MAX</sub> should still be lower than the magnetic flux density at which the core material saturates, B<sub>SAT</sub>. B<sub>MAX</sub> can be computed using Eq. (8):

$$B_{MAX} = \frac{L_{PRIMARY} I_{LIM}}{N_{PRIMARY} A_E} \quad (8)$$

The original B<sub>MAX</sub> was set to below 1500 Gauss to minimize audible noise. For this application, this performance parameter was not optimized. The peak current I<sub>LIM</sub> is set internally by the LinkSwitch-XT2 controller and an EF20 ferrite core was used. When the parameters are added to Eq. (8), we get Eq. (9):

$$1325 \text{ Gauss} = \frac{(1338 \mu H)(518 mA)}{(163 \text{ turns})(32.1 \text{ mm}^2)} \quad (9)$$

At this operating B<sub>MAX</sub>, the flyback will mostly switch at the 66 kHz maximum switching frequency during full-load operation. This, however, allows no means to address a potential drop in inductance.

To achieve a magnetic interference-resistant design, the primary inductance was doubled. As a result, the average switching frequency was lower even at the lowest input voltage. This value was selected such that the resulting increase in magnetic flux density did not cause core saturation during normal operation. It can address a potential decrease in the inductance of up to 50 percent. Because the controller utilizes an ON/OFF control scheme, no redesign was necessary. The only change is that more switching cycles would be skipped. After doubling the primary inductance in Eq. (9), the new BMAX is computed in Eq. (10):

$$2650 \text{ Gauss} = \frac{(2676\mu\text{H})(518\text{mA})}{(163 \text{ turns})(32.1 \text{ mm}^2)} \quad (10)$$

## 4. Methodology

A neodymium iron boron (NdFeB) square magnet with N35 grade, dimensions of 6.35 mm x 6.35 mm, and Gauss strength (surface Gauss) of 3451 G was placed incident to the transformer core as shown in Fig. 3.



**Fig. 3 DER-711 (TOP VIEW) with permanent magnet placed on transformer core.**

Throughout testing and performance comparison, this configuration was used. It was chosen to simulate a reduction of 50 percent of the primary inductance.

## 5. Results

### 5.1 Power Delivery

In the initial flyback design evaluation, a 50 percent reduction in the primary inductance resulted in the interruption of its operation. The initial transformer had 1338  $\mu\text{H}$  primary inductance value.

In Figs. 4 and 5 the flyback enters an auto-restart mode because it is unable to deliver output power. This was observed at both the minimum and maximum input voltage conditions.

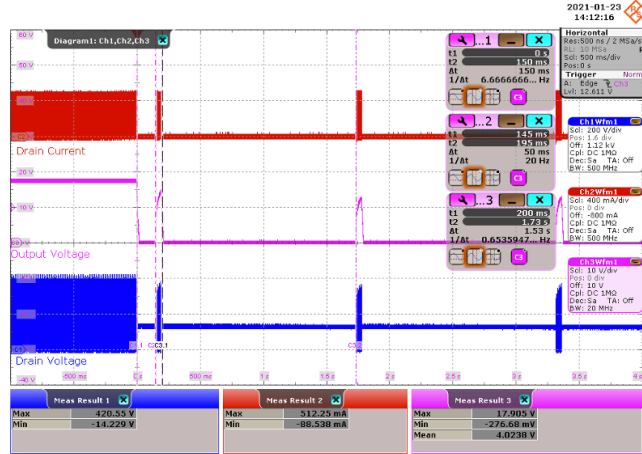


Fig. 4  $V_{IN} = 85 \text{ VAC}$ , 100 percent output load, magnet on core, power delivery was halted, part enters auto-restart,  $L_{PRI} = 1338 \mu\text{H}$

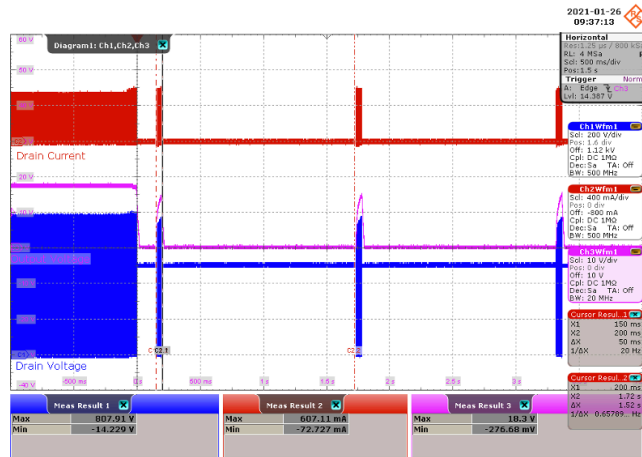


Fig. 5  $V_{IN} = 350 \text{ VAC}$ , 100 percent output load, magnet on core, power delivery was halted, part enters auto-restart,  $L_{PRI} = 1338 \mu\text{H}$

After doubling the primary inductance value, the power supply can operate despite the magnetic interference. In Fig. 6, the converter can still operate at full output load despite a reduction of the primary inductance of 50 percent.

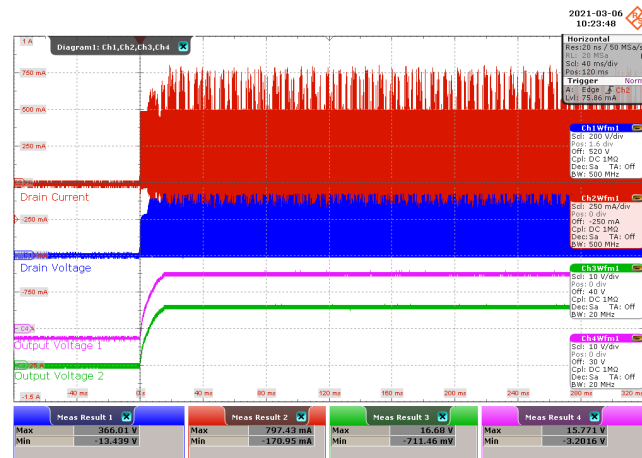


Fig. 6  $V_{IN} = 75 \text{ VAC}$ , 100 percent load, magnet on core, drain current and voltage, output voltage 1 and output voltage 2 waveforms at start-up,  $L_{PRI} = 2676 \mu\text{H}$

## 5.2 Drain Voltage and Current Waveforms

In Fig. 7, the drain current and voltage waveforms show that the average switching frequency is low. With the chosen inductance value, the ON/OFF control requests fewer switching cycles.

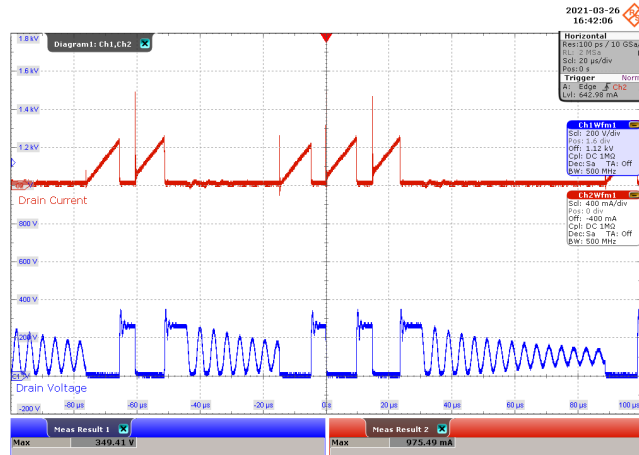


Fig. 7  $V_{IN} = 85 \text{ VAC}$ , 100 percent load, drain current and voltage waveforms

In Fig. 8, the drain current and voltage waveforms show a switching pulse at almost every cycle at 66 kHz.

Once a magnet is placed close to the transformer core, the ON/OFF control scheme would send more switching requests to the primary MOSFET detecting a change in the capability to deliver the desired output power.

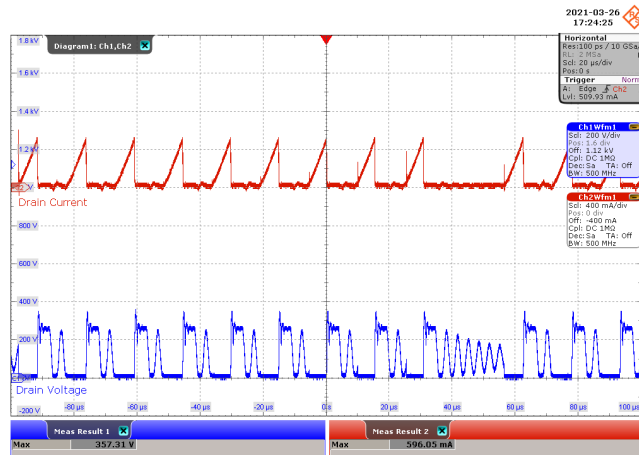


Fig. 8  $V_{IN} = 85 \text{ VAC}$ , 100 percent load, magnet on core, drain current and voltage waveforms

Also in Fig. 8, unlike in Fig. 7, we not only observe more switching cycles but also the increase in the slope of the drain current. This confirms visually the inductance drop.

### 5.3 No-Load Input Power

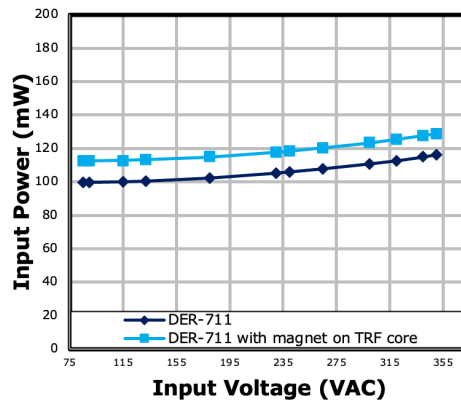


Fig. 9 No-load input power vs. input voltage

In Fig. 9, we can observe that the no-load input power increases when the magnet is placed on the transformer core. This can be attributed to more switching cycles at no-load when the inductance is suppressed by the presence of the external magnet. Despite the increase, the maximum measured no-load input power is still below the 150 mW CoC Tier 2 requirement.

### 5.4 Thermal Data After 1 Hour Soak

In Figs. 10 and 11, we can see how placing a magnet affects the temperatures of both the transformer and the power device. In Table 2, we can see the net increase in temperature for the critical components. Despite the increase, no component is above 80 °C, and the power device is well below the thermal shutdown temperature of 142 °C.

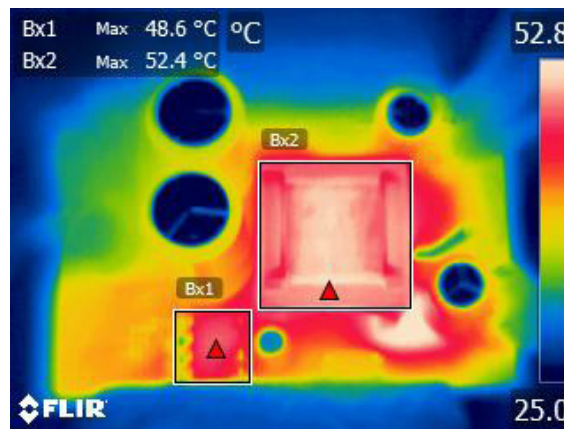


Fig. 10  $V_{IN} = 350$  VAC, thermal image, full-load operation without magnet on core

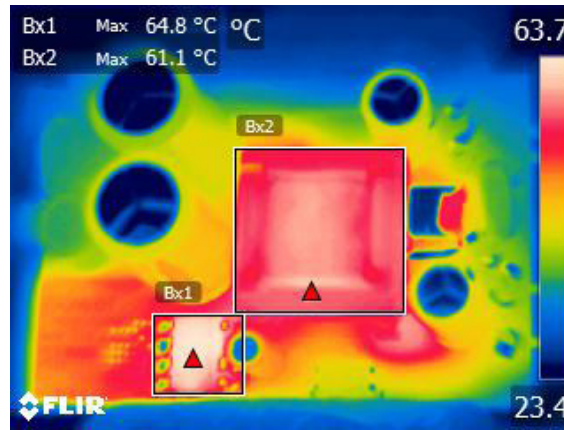


Fig. 11  $V_{in} = 350$  VAC, thermal image, full-load operation with magnet on core

Temperature	Normal operation (°C)	With magnet on core (°C)	$\Delta$ °C
Integrated device and controller	48.6	64.8	16.2
Transformer	52.4	61.1	8.7

Table 2 Temperature increase for both the integrated power device and transformer during normal operation and when a magnet is placed on the transformer core.

## 5.5 Efficiency

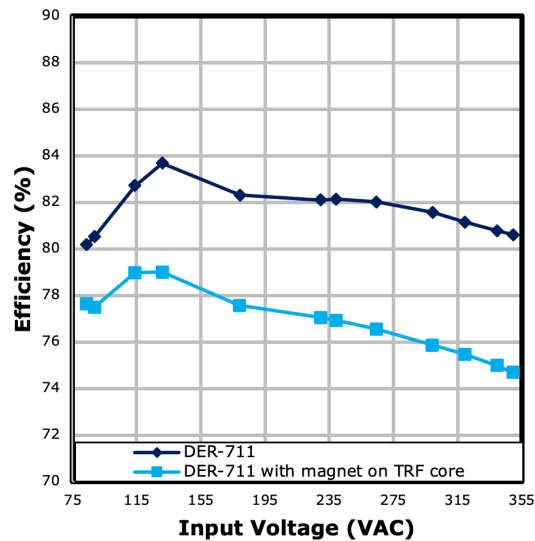


Fig. 12 Efficiency vs. input voltage

In Fig. 12, we can observe that the efficiency can drop by 6 percent at the maximum input line voltage. This again can be attributed to increased switching losses due to the increase in frequency and core loss.

## 5.6 EMI

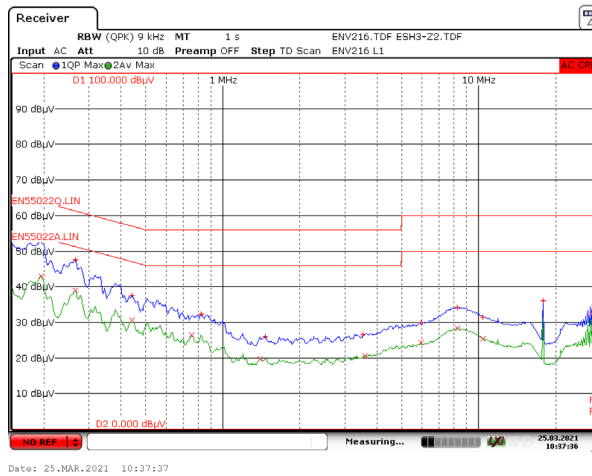


Fig. 13 EMI scan,  $V_{IN} = 230$  VAC, magnet not on transformer core

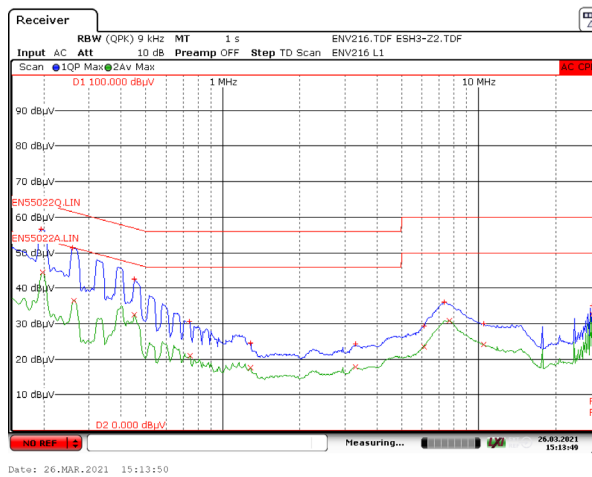


Fig. 14 EMI scan,  $V_{IN} = 230$  VAC, magnet on transformer core

Because of the lower average switching frequency, the converter is operating mostly in DCM. When the inductance is reduced, the average switching frequency increases and in both cases, the relaxation ringing of the drain voltage varies. Despite this, in Figs. 13 and 14, we can see that the EMI scan is below the requirement with sufficient margin. This is both with and without the magnet on the core.

## 6. Summary

For metering applications, this method streamlines flyback designs to guarantee power delivery despite a 50 percent reduction of the primary inductance due to magnetic interference. Increasing the target maximum magnetic flux density BMAX while still providing sufficient headroom to operate below the saturation magnetic flux density BSAT is critical.

Increasing the transformer primary inductance was the only adjustment needed. No control loop redesign was necessary because the ON/OFF control scheme had the capability to respond quickly to any change in the flyback's ability to deliver power.

The final design shows that the performance difference in the efficiency, no-load input power, thermal data, and EMI is minimal and not drastically compromised. The flyback performance with the magnetic interference was still acceptable.

The original reference design had a 6.6 W output power specification. In a separate experiment, this methodology was shown to be scalable. A reference design [2] with a 9.9 W output power specification showed similar performance. This is a 50 percent increase in output power compared to the original design and used the same power device, controller, and transformer design process.

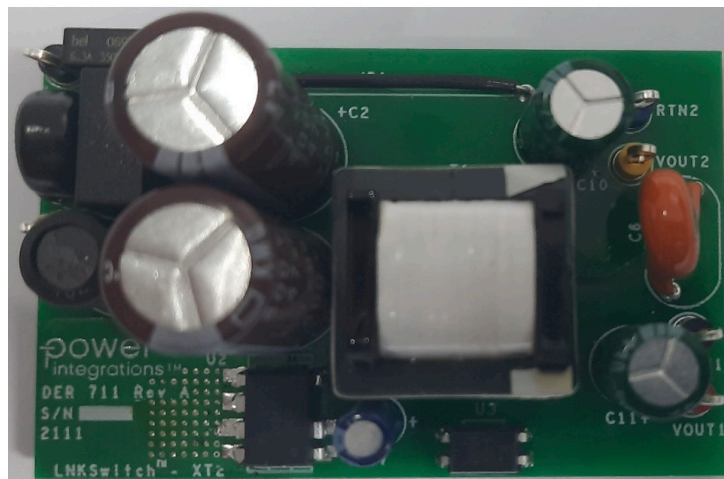


Fig. 15 DER-711, 6.6 W multi-output flyback design

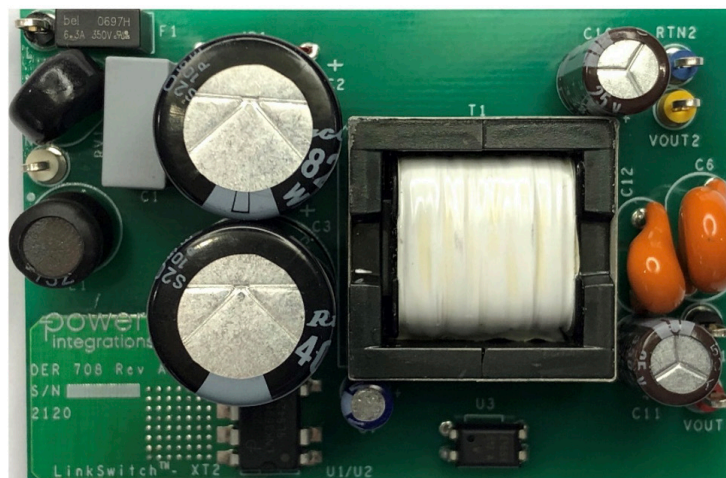


Fig. 16 DER-708, 9.9 W multi-output flyback design

---

## References

- [1] H. Young and R. Freedman, 14th Ed. University Physics with Modern Physics. New York: Pearson, 2016.
- [2] Power Integrations: “Design Example Report: 9.9 W, Wide Range Input, Dual Output, Isolated Flyback Converter for Anti-Magnetizing Interference Using LinkSwitch™ -XT2-900 LNK3696P DER-708 Date,” 2021. Accessed: Sep. 25, 2024. [Online]. Available: [https://www.power.com/sites/default/files/documents/der-708\\_9pt9watt\\_dual\\_output\\_flyback\\_anti-magnetizing\\_interference\\_for\\_metering\\_using\\_linkswitch-xt2\\_900v.pdf](https://www.power.com/sites/default/files/documents/der-708_9pt9watt_dual_output_flyback_anti-magnetizing_interference_for_metering_using_linkswitch-xt2_900v.pdf).
- [3] Power Integrations: “Design Example Report: 6.6 W, Wide Range Input, Dual Output, Isolated Flyback Converter for Anti-Magnetizing Interference Using LinkSwitch™ -XT2-900 LNK3696P DER-711 Date,” 2021. Accessed: Sep. 25, 2024. [Online]. Available: [https://www.power.com/sites/default/files/documents/der-711\\_6pt6watt\\_dual\\_output\\_flyback\\_anti-magnetizing\\_interference\\_for\\_metering\\_using\\_linkswitch-xt2\\_900v.pdf](https://www.power.com/sites/default/files/documents/der-711_6pt6watt_dual_output_flyback_anti-magnetizing_interference_for_metering_using_linkswitch-xt2_900v.pdf).
- [4] Power Integrations: “LinkSwitch-XT2 Family Energy Efficient, Low Power Off-Line Switcher IC with Integrated System Level Protection,” 2023. Accessed: Sep. 25, 2024. [Online]. Available: [https://www.power.com/sites/default/files/documents/linkswitch-xt2\\_family\\_datasheet.pdf](https://www.power.com/sites/default/files/documents/linkswitch-xt2_family_datasheet.pdf).
- [5] “Tamper-proof Isolated Flyback Power Supply for Electricity Metering AC-DC CONVERSION.” Accessed: Sep. 25, 2024. [Online]. Available: [https://www.power.com/sites/default/files/documents/Tamper-proof\\_isolated\\_flyback\\_power\\_supply\\_for\\_electricity\\_metering\\_A1021-10\\_EN\\_FINAL.pdf](https://www.power.com/sites/default/files/documents/Tamper-proof_isolated_flyback_power_supply_for_electricity_metering_A1021-10_EN_FINAL.pdf).
- [6] W. Hayt, Jr. and J. Buck, 8th Ed. Engineering Electromagnetics. New York: McGraw-Hill, 2012.

---

For more information,  
visit **power.com**<sup>™</sup>



© 2025 Power Integrations | Power Integrations, the Power Integrations logo, power.com, PowiGaN, and InnoSwitch are trademarks or registered trademarks of Power Integrations, Inc., in the U.S. and/or other countries.

050525